Atmos. Chem. Phys. Discuss., 11, 11077–11107, 2011
www.atmos-chem-phys-discuss.net/11/11077/2011/
doi:10.5194/acpd-11-11077-2011

Atmospheric Chemistry and Physics Discussions

Comparison of the size-resolved dust emission fluxes measured over a Sahelian source with the Dust Production Model (DPM) predictions

M. Sow[1,2*], **S. C. Alfaro** [1], **and J. L. Rajot**[1,2]

[1]Laboratoire Interuniversitaire des Systèmes Atmosphériques (LISA), UMR CNRS/INSU 7583, Université de Paris-Est à Créteil, Créteil, France
[2]Institut de Recherche pour le Développement (IRD), UMR IRD 211 Bioemco, Paris, France
[*]now at: Case Western Reserve University (CWRU), Cleveland, Ohio, USA

Received: 31 January 2011 – Accepted: 28 March 2011 – Published: 11 April 2011

Correspondence to: M. Sow (sowmomo2003@yahoo.fr)

Published by Copernicus Publications on behalf of the European Geosciences Union.

Abstract

This study is a follow up of Sow et al. (2009) who had used the gradient method to determine the size-resolved emission flux of 3 different erosion events monitored in natural conditions at the Banizoumbou (Niger) supersite of the African Monsoon Multidisciplinary Analysis (AMMA) experiment. Our aim is to compare these measured fluxes with the predictions of the Dust Production Model (DPM) of Alfaro and Gomes (2001), which was derived from wind tunnel experiments. For each event, the model is run using the soil aggregate dry size-distribution, soil roughness length, and wind friction velocities derived from the field measurements as input parameters. We find that the mass emission flux is correctly predicted by the model if the binding energies of the 3 populations of fine particles released by sandblasting are reduced by a factor varying between 2.5 – for the intense convective event – and 5 – for the two less energetic events of the monsoon type. We explain this need to reduce the binding energies by an underestimation of the wind velocity due to the averaging over periods of 15' required by the calculation of the wind friction velocity. In all the studied cases the emission flux can, as already assumed in the DPM, be considered as a mixture of 3 fine particle populations the proportions of which depend on the intensity of the event. However, if the geometric mean diameter (2.0 µm) of the finest population compares well to the one used in the model (1.7 µm), the values of the intermediate and coarse modes (5.0 and 10.3 µm, respectively) are smaller than previously assumed (6.7 and 14.2 µm). Finally, the amplitude of the emission does not increase with wind speed for the coarsest mode, contrary what the DPM predicts. This suggests that the scheme describing the rate at which the relative proportions of the 3 populations evolve should be revised in the model.

ACPD

11, 11077–11107, 2011

1 Introduction

It has long been recognized that the mineral particles released by wind erosion in arid and semi arid areas alter the atmospheric transfer of solar and terrestrial radiation directly, by scattering and absorbing photons (Kaufman et al., 2002), and possibly indirectly by favouring the formation of clouds or modifying their properties (Levin et al., 1995). Among the uplifted particles, the smallest ones (those with sizes <20 µm, hereinafter referred to as PM_{20}) are the most optically active. They are also those most prone to remain suspended for a long time (up to a week in the lower troposphere) and can therefore be entrained very far from their sources. The departure of nutrient-enriched fine dust from the usually poor soils of semi-arid areas can also promote desertification of the source areas (Bielders et al., 2001; Li et al., 2009). Quantification of the emission strength as well as assessment of the size-resolved concentration-fields of the transported particles are crucial for the estimation of the various impacts of mineral dust. Practically, emission fluxes and size-resolved concentrations are calculated using transport/deposition models inside which schemes describing the emission processes are imbedded. Among these schemes, very few provide at the same time the intensity and the initial size distribution of the emission flux. One of them – the "dust production model" or DPM – was proposed by Alfaro and Gomes (2001) and is in fact a combination of two sub-models: the first one developed by Marticorena and Bergametti (1995) describes the setting into motion of loose soil-aggregates (saltation) by the stress exerted by the wind on the surface, and the second one accounts for the release of PM_{20} (sandblasting) from these aggregates when they hit the soil at the end of their ballistic jumps. The sandblasting theory underlying this second model was itself derived from erosion simulations performed in a laboratory wind tunnel (Alfaro et al., 1997, 1998). One of the most striking results of these experiments was that the emission flux was richer in the finest PM_{20} particles at high wind speeds than at velocities just above saltation threshold. This was interpreted by considering (1) that the binding energy of the PM_{20} particles within the soil aggregates is a decreasing function of their

ACPD
11, 11077–11107, 2011

size, and (2) that the proportion of the very fine PM_{20} modes increased with the kinetic energy of the saltating sand grains. Until quite recently, there was a complete lack of sufficiently detailed field observations to confirm this new finding that the initial size distribution of the dust flux was not independent of the aerodynamic conditions prevailing during the dust event. The only data available for the validation of the DPM were non size-resolved mass fluxes obtained by measuring wind velocity profiles and particle concentrations at two different elevations in the surface boundary layer and applying to them the so-called gradient method proposed by Gillette et al. (1972). Moreover, the time resolution of this method was relatively poor. Indeed, particle concentrations were determined from the mass of particles accumulated on filters during sampling periods of typically 1 h at least, which is a long time in comparison with the instantaneous fluctuations of wind intensity during an erosion event. Nonetheless, when using the results of masse fluxes measurements performed over a variety of bare agricultural surfaces located either in the south-western part of the USA (Nickling and Gillies, 1989), in northern Spain (Gomes et al., 2003), or in Niger (Rajot et al., 2003), Alfaro et al. (2004) showed that the DPM was able to predict correctly the intensity of the emission flux provided if the binding energies of the PM_{20} within the soil aggregates as derived from the wind tunnel experiments were divided by a factor β larger than 1. Though the reason for this was not understood, this seemed to suggest that the fine particles were easier to release in natural conditions than in the laboratory simulations. During the 2006 and 2007 special observation periods of the African Monsoon Multidisciplinary Analysis (AMMA), a new methodology was designed and set up on an African field in Banizoumbou (Niger) for measuring simultaneously, and with a time resolution of 1 min, the intensity and the size distribution of the emission flux (Sow et al., 2009). Practically, two sampling heads were used to measure each minute the size-resolved dust concentration at 2m and 6m above ground. The size-resolved emission flux was then obtained by the means of the concentration difference between the two levels combined with the aerodynamic parameters u^* and z_0 according to the gradient method. Note that if a size-resolved emission flux was calculated for each minute, this

ACPD
11, 11077–11107, 2011

one was obtained using a value of u^* which was a sliding average over periods of 15' as required by the calculation of this parameter. After a rigorous data qualification phase, we analyzed the data collected during 3 different, fully-documented erosion events and their results confirmed for the first time the laboratory finding stipulating that the emission flux was proportionally richer in very fine particles during the strong erosion event than during the moderate ones. The aim of the present work, which is a follow up of this previous study, is to assess quantitatively the ability of the DPM to predict the characteristics of the emission flux for the wind and soil conditions of the 3 aforementioned erosion events. It is organized as follows: next section describes the principles of the method we propose for achieving our goal. In particular, the nature of the input data necessary for running the DPM and how they can be derived from the field measurements is reminded. The following "results and comments" section constitutes the core of this work. It compares the predictions of the DPM with the direct measurements first in terms of mass flux, then in terms of size-resolved flux. In each case, the reasons for the discrepancies between predicted and measured fluxes are carefully analyzed.

2 Methods

The principle of the validation of the DPM consists in comparing the mass fluxes and the size-resolved fluxes calculated using the model with the fluxes measured independently on the field. Naturally, this comparison exercise is possible only for eroding periods during which all the input data necessary for running the DPM and the characteristics of the emission flux have been measured simultaneously. The 3 erosion events reported previously by Sow et al. (2009) respect these conditions. The first two events (ME1 and ME4) occurred during the 2006 AMMA special observation period (SOP1), lasted approximately 2 h and 40 min (respectively), and were classified as events of the monsoon type because they were due to a temporal strengthening of the southwestern winds typical of the monsoon season. These events were also relatively moderate as compared to the third event (CE4), which was observed during the

ACPD
11, 11077–11107, 2011

2007 AMMA SOP due to a passing convective system. This event was not only more energetic than ME1 and ME4, it also lasted significantly longer (2 h 44 min).

During the 3 events, a meteorological mast instrumented with a wind vane, 5 anemometers and 4 temperature probes measured the wind and temperature profiles necessary for the computation of both the wind friction velocity (u^*) and soil roughness length (z_0). As described in more detail in Sow et al. (2009), a value of u^* and z_0 is available for each minute of the events but the calculation of these two parameters involves an averaging of the measurements over periods of 15 min. Beside u^*, which quantifies the stress exerted on the ground by the aerodynamic flow, the importance of saltation also depends on the dry size distribution of the loose aggregates present on the soil surface and on z_0, which is used for parameterizing the degree of protection brought to sand-sized grains by elements too large to be moved by the wind (Alfaro and Gomes, 1995). Practically, the size distribution of the erodible fraction of the soil is determined by sieving in dry conditions samples collected on the field during the 2007 AMMA field campaign and by applying the fitting procedure of Gomes el al. (1990) to the results to obtain the parameters (amplitude, geometric mean diameter, and geometric standard deviation) of the log-normally distributed particle populations fitting best the measurements.

In parallel with this determination of the DPM inputs, the particle mass concentrations necessary for the quantification of the emission flux by the gradient method were measured with two automated microbalances (TEOM, model 1400a, Rupprecht and Pataschnik, Albany, New York, USA) with an acquisition time of 2 min and connected to two inlets located at 2.1 and 6.5m above the emitting surface (Rajot et al., 2008). Two identical particle-sizers (GRIMM, OPC 1.108, GRIMM Aerosol Technik Gmbh & Co., Ainring, Germany) were also connected to the same inlets and measured the particle concentrations in 15 size-classes between 0.3 and 20 µm, providing in turn the possibility of computing the size-resolved number emission flux by application of the gradient method to each individual size class. For more details on the flux determination, we refer the reader to the previous work of Sow et al. (2009). Note that these authors

ACPD
11, 11077–11107, 2011

also checked the consistency between the mass and size-resolved fluxes determined independently.

3 Results and comments

3.1 Model input for the 3 studied events

3.1.1 Size distribution of the erodible loose particles

The analysis of the dry soil samples collected on the surface of the Banizoumbou field during the 2007 experiment show that the soil aggregates can be considered as a combination of 3 different log-normally distributed populations whose amplitudes (A), geometric mean diameters (gmd), and geometric standard deviations (σ) are reported in Table 1. When considered together, the two finer populations (pop 1 and pop 2) account for as much as 97% of the total mass and correspond to grains which can be easily mobilized by the wind. This confirms the quite erodible nature of the Banizoumbou sandy agricultural field over which the AMMA experiment was conducted. Conversely, the third population (pop3, with a gmd of 3mm) represents a negligible proportion (3%) of the mass and corresponds to a limited number of coarse iron oxide rich grains dispersed at the surface of the field. When observed under an optical microscope, the vast majority of the sand grains appear to be quartz grains at the surface of which the very fine PM_{20} particles are stuck. Because any inter-annual significant change in the size of the quartz grains is unlikely, the size distribution of the sand grains will be assumed to be identical in 2006 and 2007. In other words, the size distribution parameters reported in Table 1 will be those used as direct inputs for all the model simulations.

ACPD
11, 11077–11107, 2011

3.1.2 Aerodynamic parameters

Soil roughness length

As reminded above, the wind friction velocity u^* and the aerodynamic roughness length z_0 are derived simultaneously from the analysis of the wind and temperature profiles monitored during the 3 erosion events. The surface roughness is highly sensitive to the presence, and to the spatial distribution, of non-erodible elements (crop residue, shrubs, trees ...) on the soil surface and a simple visual observation of the millet field in which our system was implemented revealed that these roughness elements were not evenly distributed. Due to this anisotropy, one expects that z_0 might depend at least to a degree on wind direction, as was previously reported by Rajot el al. (2003) for a different field in the same area. This is indeed what is observed (Fig. 1). Because wind blew from different directions during the two 2006 monsoon events, the range of z_0 values during ME4 is one order of magnitude lower than during ME1. Also note that for comparable directions, z_0 is larger during the convective event of 2007 (CE4) than during ME1. This suggests that the rearrangement of sand masses at the surface of the field due to the successive erosion events, the effect of the agricultural practices including weeding during the rainy season, and most importantly the quality of the crop conditioning the amount of crop residues (Abdourhamane Toure et al., 2011), could create a new surface micro-morphology for each season. In summary, unlike what was assumed for the size-distribution of the sand grains, it is impossible to assign a unique z_0 value to the whole millet field. Therefore, in the model calculations of the emission flux we will use the average values of z_0 corresponding to each individual erosion event (Table 2).

ACPD
11, 11077–11107, 2011

Wind friction velocity and its statistical distribution during the three studied events

By definition, an erosion event corresponds to a period when the instantaneous wind speed becomes larger than the threshold value necessary to initiate the saltation. During this period, the movement of sand grains responds almost instantaneously to the fluctuations of the stress exerted by the aerodynamic flow on the soil surface (Stout et al., 1998). Usually, the models used to simulate saltation do not use instantaneous wind speeds as input parameters but rather the friction velocity whose value is the result of an averaging over periods of at least 15 min (see above). Because saltation is a non-linear process whose intensity increases much faster than wind speed, this averaging might lead to an underestimation of the quantitative role played by the very short, but intense, wind peaks. This remark being made, the range of values encompassed by u^* and the statistical distribution of these values are also key factors for the estimation of the cumulated sand movements and of the subsequent dust emission due to a given erosion event. The principle of the analysis of this distribution is going to be detailed for CE4, and then applied to ME1 and ME4.

During CE4, the wind friction velocities responsible for sand movements ranged from the threshold of saltation (0.45 m s^{-1}) to a maximum of 0.77 m s^{-1}. The distribution of these u^*-values into bins of fixed width (=0.05 m s^{-1}) is clearly bi-modal (Fig. 2) and can be conveniently approximated using a combination of 2 velocity modes of the Gaussian type:

$$g(u*) = \frac{\mathrm{B}}{\sigma\sqrt{2\pi}} \exp[-0,5(u^* - U^*/\sigma)^2] \quad (1)$$

In this classical expression B is the amplitude (i.e., the number of u^* values belonging to the mode), u^* the mean friction velocity, and σ the standard deviation. The unknown values of these parameters can be obtained using an iterative least-square routine aiming at minimizing the difference between the actual (measured) distribution and its mathematical expression. Results obtained for CE4 are reported in Table 2.

ACPD
11, 11077–11107, 2011

When applied to the two monsoon events, the same method shows (Table 2) that the distribution of u^* values is also bi-modal (modes centered on 0.33 and 0.50 m s^{-1}) during ME4 but simply mono-modal (centered on 0.45 m s^{-1}) in the case of ME1. Noteworthy is the presence of a mode of intense friction velocities centered on 0.67 m s^{-1} during CE4. This mode, not observed during the two events of the monsoon type, contributes as much as 56% of the total number of observations. The implications of the differences in u^* distributions for the 3 erosion events are now going to be assessed more precisely.

3.2 Saltation flux for the 3 studied events

The size-distribution of loose aggregates at the soil surface, the aerodynamic roughness length, and the statistical distribution of u^* constitute the inputs of the saltation model proposed by Marticorena and Bergametti (1995). Therefore, it is possible to calculate the intensity of the saltation flux cumulated over the duration of each event. The contribution of any specific u^* value to the total flux can also be assessed. Unsurprisingly, the largest u^* values are found to contribute significantly more to the sand movements than values just above saltation threshold (Fig. 3). In particular, in the case of CE4 and ME4 whose wind distributions were bi-modal, the largest wind mode contributes as much as 95 and 98% of the total saltation flux, respectively. Another consequence of the non-linearity of the saltation process is the narrowness of the distribution of the saltation flux as compared to the width of the distribution of u^*-values (Fig. 3). The saltation flux can be considered as practically monomodal and centred on a friction velocity value slightly larger than the mean of the highest u^*-mode. On figure 3, this shift of the saltation flux distribution towards large u^*-values is also observed very clearly in the case of ME1 in spite of its monomodal nature. Note that the limited range of u^* values contributing really efficiently to the saltation flux probably explains the field observation by Sow et al. (2009) that the size distribution of the emission flux remained relatively stable within a given erosion event, and this in spite of relatively important fluctuations of the friction velocity. Practically, the wind friction velocity on which the

ACPD
11, 11077–11107, 2011

distribution of the saltation flux is centred plays a crucial role in the determination of the characteristics of the emission flux. We define this value as the "equivalent wind friction velocity" (u^*_{eq}) of the event. For instance, with a saltation mode centred on a friction velocity of about 0.70 m s^{-1}, the breakage of saltating soil-aggregates is expected to be more efficient during CE4 than during ME1 and ME4 whose saltation modes are both centred on smaller wind friction velocities close to 0.50 m s^{-1}. In turn, this also explains that the dust emission flux was found to be richer in submicron particles during the convective event than during the 2 monsoon ones (Sow et al., 2009).

Finally, the influence of z_0 on the sand movements can be illustrated by calculating the intensity of saltation for the largest wind modes of each of the 3 events. At 0.67 m s^{-1} for CE4, 0,50 m s^{-1} for ME4, and 0,45 m s^{-1} for ME1, the horizontal fluxes calculated with the saltation model of Marticorena and Bergametti (1995) are 0.297 g cm^{-1} s^{-1}, 0.145 g cm^{-1} s^{-1} and 0.078 g cm^{-1} s^{-1} respectively. The roughness length being about one order of magnitude smaller during ME4 than during ME1 (Table 2) explains that in spite of similar u^* values, the horizontal flux is approximately two times larger during ME4 than during ME1.

3.3 Comparing the simulated and measured PM_{20} emission fluxes

3.3.1 Vertical mass flux

The integrated mass flux of fine particles can be calculated using the DPM with the input data already listed for the saltation (soil size distribution, z_0, and u^*), the size characteristics of the three modes of particles which can be released by the sandblasting process, and the values of the binding energies required by the sandblasting module. In the DPM, the characteristics of the 3 PM_{20} modes are assumed to be universal which is also supported by the complementary wind tunnel experiments of Alfaro (2007) in which it was shown that the size distribution of the fine dust released by sandblasting seemed to be largely independent of the texture and mineralogical composition of the parent soil. Therefore, the gmd and gsd used in this work have the values of Alfaro

ACPD
11, 11077–11107, 2011

and Gomes (2001). The binding energies are also derived from the wind tunnel experiments but as proposed by Alfaro et al. (2004) their original values are divided by a tuning factor (β). Indeed, these last authors found that the best agreement between the dust emission fluxes measured above a variety of agricultural surfaces and the model predictions was obtained for $\beta = 3$. In the present work, β not fixed a priori and the vertical mass fluxes calculated with different values of this parameter are compared to the field measurements (Sow et al., 2009) obtained by applying the gradient method to the mass concentrations measured with the two TEOM microbalances at two different levels inside the surface boundary layer. The best agreement is obtained with $\beta = 5$ (± 1) for ME1 and ME4, and with $\beta = 2.5$ (± 0.5) for CE4 (Fig. 4). Note that though this last value is closer to the one proposed by Alfaro et al., the fact that β is larger than 1 in all the tested cases confirms the need to reduce systematically the binding energies derived from the wind tunnel experiments for simulating properly the intensity of the emission flux with the DPM. A tentative explanation for this difference could be the following: in each wind tunnel experiment the wind conditions were fixed and the friction velocity was thus maintained constant. Conversely, wind speed fluctuates rapidly on the field and, due to the smoothing effect of the averaging over durations of 15 min, the experimental values of u^* underestimate the effect of the largest wind values achieved during the averaging period. In order to counterbalance this misrepresentation of the most efficient wind speeds by u^*, the values of the binding energies must be artificially reduced (i.e., divided by a $\beta > 1$) for the model to remain able to reproduce the observed emission intensities at their real level. In addition, because saltation increases much more rapidly with wind speed just above threshold than at larger velocities, the underestimation of the contribution of the strongest winds in each 15'-period is expected to be relatively more important during the moderate events than during the energetic ones. In turn, this could explain why the binding energies reducing factor is smaller during the convective event ($\beta = 2.5$) than during the ones of the monsoon type ($\beta = 5$).

ACPD
11, 11077–11107, 2011

Independently of this question of the binding energies, the integration of the mass flux over the duration of each event provides a mean of quantifying the cumulated loss (L) of PM_{20} particles by each square meter of the source. By dividing L by the duration of the emission, an average flux ($F_{v,\mathrm{av.}}$) can also be calculated for the 3 events. Results (Table 2) show that in spite of the important friction velocities achieved during CE4, the average flux during this event (1.01 mg m^{-2} s^{-1}) is slightly smaller than during ME1 (1.11 mg m^{-2} s^{-1}), and most particularly than during ME4 (1.50 mg m^{-2} s). As already commented above, this can be explained at least in part by the important soil roughness limiting saltation during CE4, and probably also by the fact that, as compared to the monsoon events, the emission flux is enriched in the finest mode of sandblasted particles during the convective event. More precisely, that a significant proportion of the kinetic energy of the saltating sand grains is used to release the lightest particles during CE4 results in a limitation of the mass efficiency of the sandblasting process. Finally, the cumulated source loss is larger during CE4 (10.5 g m^{-2}) than during ME1 and ME4 (8.6 and 3.5 g m^{-2}, respectively) only because of the particularly long duration of CE4

3.3.2 Size-resolved flux

As reminded above, Sow et al. (2009) found that although the intensity of the emission flux fluctuated in the course of a given erosion event, its relative size distribution remained fairly stable. As a result of this constancy, these authors used the averages of the size-resolved flux calculated over the durations of the 3 studied events for comparing their size distributions. Whether expressed in terms of a number of particles or of in terms of a mass released each second by a surface unit of field, these experimental fluxes can be compared to the fluxes predicted by the DPM at increasing u^*-values. Note that, in the calculations, the values chosen for z_0 and β (5 for ME1 and ME4, and 2.5 for CE4) were those determined previously for each event. The results (Fig. 5) of this comparison clearly emphasize some discrepancies between the model predictions and the measurements. More precisely, 4 behaviours correspond-

ACPD
11, 11077–11107, 2011

ing to 4 different size ranges can be distinguished. The first size range corresponds to particles with diameters between 0.40 and approximately 1 µm: for this range, the model is able to simulate the average flux provided a suitable value of u^* is selected. This value is found to be approximately 0.50 m s^{-1} for ME1, between 0.45 and 0.50 for ME4, and close to 0.75 m s^{-1} for CE4. The fact that these values coincide almost exactly with the highest modes of the distribution of the saltation flux emphasizes again the out-of-proportion influence of a narrow range of large u^* values when it comes to determining the characteristics of the emission flux. In the submicron range, the smallest size class (0.30–0.40 µm) of the optical counter used for the concentration measurements constitutes a notable exception. Indeed, the corresponding measured flux is systematically larger than predicted by the DPM. A first possible explanation for this could be that a population of submicron particles centred on a diameter smaller than 0.30 µm and not accounted for by the model is produced by the sandblasting process. Another completely different possibility would be that the optical counter is able to actually see particles smaller than the theoretical lower limit (0.30 µm) of its smaller size class and that it distributes these particles unduly in the 0.30–0.40 µm range, thus leading to an artificial overestimation of the concentrations and consequently of the emission flux in this particular size-class. Because no particle counter able to detect and size efficiently particles smaller than 0.30 µm was operated at the Banizoumbou experimental site, it is not possible to arbitrate between these two options.

Regarding the model predictions, the behaviours of the 2–8 µm and >8 µm diameter ranges are completely different. More precisely, whatever the value selected for u^* the model underestimates the flux measured in the first range and overestimates it in the second. The overestimation of the emission of coarse (>8 µm) particles by the model is visible on the number flux representation but is even more obvious on the mass plots of Fig. 5. Indeed, examination of the latter reveals that for the 3 events a maximum of the measured flux is obtained for diameters between roughly 5 and 10 µm, whereas the DPM predicts a maximum around 14 µm – a value corresponding to the geometric mean diameter of the coarsest population of particles detected in the

ACPD
11, 11077–11107, 2011

wind tunnel measurements of Alfaro et al. (1998). Comparing the mass plots of the 3 events shows that the overestimation of the emission of particles >8 µm by the model is more pronounced in the case of CE4. In this convective case, the overestimation of the mass emission flux by the model is larger than in the monsoon-type events, which is also consistent with a smaller value of the β factor being necessary to simulate correctly the CE4 mass emissions. Note that in the 3 cases, a good estimate of the total mass flux could be achieved only because of a compensation effect between the overestimation of the coarsest particles and an underestimation of the particles in the medium (2–8 µm) size-range. This also suggests that the geometric mean diameter (gmd) and geometric standard deviation (gsd) of the populations of fine particles whose mixture constitutes the emission flux in Banizoumbou might not be the same as the ones derived from the wind tunnel experiment. In particular, the 14 µm gmd of the coarsest mode seems to be too large in view of the measured size-resolved emission flux. The next section aims at assessing more precisely the characteristics of the PM_{20} populations most able to explain the observed size distributions during the 3 studied events.

3.4 Deconvolution of the measured emission fluxes

Basically, the analysis of the measured size-resolved flux is done following the same deconvolution procedure as the one used by Alfaro et al. (1998) in their laboratory study of the sandblasting process. In brief, the normalized size resolved emission flux is considered as being a mixture of a certain number (N) of lognormally distributed particle populations, which is tantamount to saying that it is well represented by:

$$\frac{dF_v}{d\log d} = \sum_{j=1}^{N} \frac{A_j}{\sigma_j \sqrt{2\pi}} \exp\left[-\frac{(\ln d - \ln d_j)^2}{2\sigma_j^2}\right] \quad (2)$$

In this expression, the proportions of each population in the mixture (A_j, in %), their gmd (d_j), and their gsd (σ_j) are initially unknown. These parameters are retrieved

ACPD
11, 11077–11107, 2011

using the method of Gomes et al. (1990), which is based on an iterative least square routine aiming at minimizing the difference between the measured flux and the one calculated with Eq. (2). Note that the procedure can be applied indifferently to the mass or number size-resolved fluxes. In this work, the smallest size-class (0.30–0.40 µm) is ignored in the deconvolution because of the uncertainties attached to it (see above) but both the mass and number distributions are used in order to increase the precision of the method over the whole range (0.40–20 µm) of other available sizes. Indeed, mass size distributions are mostly sensitive to the presence of coarse (supermicron) particles and very little to the submicron ones. Conversely, these very fine particles are better accounted for by the number distributions. Fig. 6 illustrates the quality of the deconvolution procedure with the case of the convective event, and Table 3 summarizes the results obtained for the 3 events and for both the mass and number size-distributions.

During each of the 3 events, 3 populations of PM_{20} with gmds ranging from 2.0 to 10.3 µm must be combined in order to reproduce correctly the emission flux. The results of the deconvolution also confirm quantitatively the qualitative findings of Sow et al. (2009); namely, that the relative proportion of the smallest PM_{20} population (pop. 1) is larger in the case of the convective erosion event. In these energetic conditions, the contribution of the largest population (pop. 3) to either the number or mass flux (<1% and 8%, respectively) is also found to be small. This weakness of the share of the coarsest particle mode is reflected in the enhancement of the relative proportion of the smallest population (pop. 1) in the emission flux. Qualitatively, these findings are in good agreement with the wind tunnel experiments and the sandblasting theory deduced from them, showing that the proportion of the finest particles should increase with the kinetic energy of the saltating sand grains. However, several numerical discrepancies can also be observed. In particular, if the average gmd (2.0 µm) of pop.1 compares relatively well to the one (1.5 µm) of the finest population of Alfaro et al. (1998), this is not the case for the coarsest (pop. 3) and intermediate (pop. 2) populations whose gmds (10.3 and 5.0 µm, respectively) are significantly smaller than those (14.2 and 6.7 µm) derived from the wind tunnel experiments. Although this should

ACPD
11, 11077–11107, 2011

be further investigated, this difference could be due to instrumental reasons. Indeed, in the laboratory simulations, the particle size distributions were measured with a laser particle analyzer (Malvern Mastersizer) sorting particles into 32 size classes ranging from 1.2 to 600 µm. The measurement range and resolution (15 size-classes between 0.3 and 20 µm) of the Grimm optical particle sizer (OPS) used in the field experiment are better adapted to the sizes of the particles produced by the sandblasting process and, consequently, a better accuracy is expected for the inversion of the size-resolved flux measured by the OPS . In any case, the different positioning of the medium and coarse modes derived from the wind tunnel experiments seems to explain on the one hand the overestimation of the contribution of the particles coarser than 10 µm to the emission flux, and on the other hand the underestimation of the contribution of particles with diameters between 2 and 8 µm. Replacing in the DPM the wind tunnel-derived gmds and gsds by the new average values proposed in Table 3 would certainly help improve the agreement between the predicted size-resolved fluxes and those measured at the Banizoumbou experimental site. However, another question arises on examination of the amplitudes of the coarsest population (pop. 3) presented in Table 3. This examination reveals that their order of magnitude is the same for the 3 events. In particular, contrary to what is predicted by the DPM, this amplitude is not more important during the convective event than during the two monsoon ones. This suggests the existence of some sort of saturation effect in the release of the coarsest mode of particles which is not accounted for by the DPM. More generally, the rhythm at which the size-distribution of the emission flux shifts towards the finest diameters as u^* increases must be revised in the model. Although some quantitative information as to this rhythm is provided by the proportions of the modes given in Table 3, the number of events fully documented on the field – only 3 among which ME1 and ME4 are very close in terms of dominating friction velocities ($u^* = 0.45$ and $0.5\,\mathrm{m\,s^{-1}}$, respectively) – is too limited for inferring a new empirical law describing accurately the rate at which the proportions of the 3 populations of fine particles evolve in the emission flux.

ACPD
11, 11077–11107, 2011

4 Summary and conclusion

In the frame of the 2006 and 2007 intensive observation periods of the AMMA experiment, measurements aiming at documenting the characteristics of local erosion have been performed at the Banizoumbou (Niger) supersite (Sow et al., 2009). During the course of three different erosion events – two moderate ones of the monsoon type (ME1 and ME4) and a more energetic one of the convective type (CE4)-, the dry size-distribution of the loose soil-aggregates available for saltation was determined and the meteorological measurements necessary for retrieving the soil roughness length and the wind friction velocity were performed. For these three events, the experimental values of the intensity and size-distribution of the emission flux determined previously by Sow et al. (2009) are also available. Therefore, field measurements performed in natural conditions provide simultaneously, and this for the first time, all the (1) input parameters necessary for running the Dust Production Model (DPM) of Alfaro and Gomes (2001), and (2) the outputs of the model. In this work, we use this unique dataset for testing the accuracy of the predictions of the DPM.

In a first step, we compared the intensity of the calculated mass emission flux with the one measured onsite during the three erosion events. In each case a very good agreement can be obtained between the model predictions and the measurements. However, as already suggested by Alfaro et al. (2004), this agreement can only be achieved if the binding energies of fine particulate modes potentially released from the soil aggregates by the sandblasting process are significantly reduced. We explain this necessity by the fact that the calculation of the friction velocity (u^*) used as an input parameter of the model includes an averaging over a period of 15', which is a long time as compared to the typical response time of sand movements. The smoothing effect of this averaging leads to an underestimation of the effect of the largest wind values and, because the wind peaks are the most efficient in the erosion process, the underestimation of their effect must be compensated artificially in the model by increasing the facility with which the PM_{20} are released. This is done by dividing the corresponding

ACPD
11, 11077–11107, 2011

binding energies by a factor β ($\beta > 1$). Regarding this point, it is also because saltation increases much faster with wind speed just above threshold than at larger velocities, that the need to tune down the binding energies is larger in the moderate events of the monsoon type ($\beta = 5$) than during the more energetic convective event ($\beta = 2.5$).

In a second step, we have compared the size-resolved emission fluxes measured on the field with those predicted by the DPM at increasing values of u^*. Results of these comparisons show that for particles with diameters between 0.4 and 1 µm, the fluxes calculated using a friction velocity (u^*_{eq}) close to the mean value of the largest mode of the statistical distribution of u^*, are in good agreement with the measured ones. This emphasizes again the out-of-proportion role played by the wind peaks and the importance to take them into account in the modeling of the characteristics of the emission flux. In the submicron range, the smallest size-class (0.3–0.4 µm) of the optical counter used for measuring the particle concentrations on the field constitutes an exception to the previous agreement. For lack of experimental data, it is not possible to ascertain whether the enhancement of the flux measured in this particular size class is really due to the emission of a population of particles centered on a diameter smaller than 0.3 µm or to a systematic overestimation by the instrument of the particle concentrations in its smaller size-class. In the supermicron range of sizes more important discrepancies are observed between the model outputs and the measured fluxes. Indeed, if the reanalysis of the size-distribution of the measured fluxes confirms the laboratory findings indicating that the emission flux is a mixture of three particles populations the smaller of which has a geometric mean diameter (2.0 µm) that compares well to the one (1.5 µm) recommended by Alfaro and Gomes (2001), the gmds of the two other populations are smaller (5.0, and 10.3 µm) than the values (6.7 and 14.2 µm) previously derived from the wind-tunnel measurements.

The rhythm at which the three modes of particles are released also needs to be revised in the model. In particular, observations show that the amplitude of the flux associated with the coarsest mode is not significantly larger during the energetic convective event than during the two more moderate monsoon ones. This sort of saturation

ACPD
11, 11077–11107, 2011

effect, which is not accounted for by the DPM in its current state suggests either that there is a supply limitation of the coarsest mode of PM_{20} particles in the Banizoumbou soil-aggregates, or that these coarse particles are themselves able to disintegrate into particles of the two finest modes at large wind speeds. Complementary experimental work will be necessary to decide which of these two options is the more realistic.

Acknowledgements. Based on a French initiative, AMMA was built by an international scientific group and is currently funded by a large number of agencies, especially from France, UK, US and Africa. It has been the beneficiary of a major financial contribution from the European Community's Sixth Framework Research. The authors are also grateful to all the persons from the IRD and LISA who have made the experiment possible first by setting up the experimental site and subsequently by servicing it in difficult conditions during the two intensive observation periods of 2006 and 2007. They also thank the "Institut National des Sciences de l'Univers" (INSU/CNRS) for his support.

The publication of this article is financed by CNRS-INSU.

References

Abdourhamane Toure, A., Rajot J. L., Garba, Z., Marticorena, B., Petit, C., and Sebag, D.: Impact of very low crop residues cover on wind erosion in the Sahel, Catena, 85:205–214, doi:10.1016/j.catena.2011.01.002, 2011

Alfaro, S.C.: Influence of soil texture on the binding energies of fine mineral dust particles potentially released by wind erosion, Geomorphology, 93, 3–4,157–167, doi:10.1016/j.geomorph.2007.02.012., 2008.

ACPD

11, 11077–11107, 2011

Alfaro, S. C. and Gomes, L.: Improving the large-scale modelling of the saltation flux of soil-particles in presence of non erodible elements, J. Geophys. Res., 100, 16357–16366, 1995.
Alfaro, S. C. and Gomes, L.: Modelling mineral aerosol production by wind erosion: Emission intensities and aerosol distributions in source areas, J. Geophys. Res., 106, 18075–18084, 2001.
Alfaro, S. C., Gaudichet, A., Gomes, L., and Maillé, M.: Modelling the size distribution of a soil aerosol produced by sandblasting, J. Geophys. Res, 102, 11239–11249, 1997.
Alfaro, S. C., Gaudichet, A., Gomes, L., and Maillé, M.: Mineral aerosol production by wind erosion: aerosol particle sizes and binding energies, Geophys. Res. Lett, 25(7), 991–994, 1998.
Alfaro, S. C., Rajot, J. L., and Nickling, W.: Estimation of PM_{20} emissions by wind erosion: Main sources of uncertainties, Geomorphology, 59, 63–74, 2004.
Bielders, C. L., Alvey, S., and Cronyn, N.: Wind erosion: The perspective of grass-roots Zcommunities in the Sahel, Land Degrad. Dev., 12(1), 57–70, 2001.
Gillette, D., Blifford, I. H., and Fenster, C. R.: Measurements of aerosol size distributions and fluxes of aerosols on land subject to wind erosion, J. Appl. Meteorol., 11, 977–987, 1972.
Gomes, L., G. Bergametti, G. Coudé-Gaussen, and Rognon, P.: Submicron Desert Dusts: A Sandblasting Process, J. Geophys. Res., 95(D9), 13,927–13,935, doi:10.1029/JD095iD09p13927, 1990.
Gomes, L., Rajot, J. L., Alfaro, S .C., and Gaudichet, A.: Validation of a dust production model from measurements performed in semi-arid agricultural areas of Spain and Niger, Catena, 52, 257–271, 2003.
Kaufman, Y. J., Tanré, D., and Boucher, O.: A satellite view of aerosols in the climate system, Nature, 419, 215–223, 2002.
Levin, Z., Ganor, E., and Gladstein, V.: The effect of desert particles coated with sulfate on rain formation in the Eastern Mediterranean, American Meteorological Society, 35, 1511–1523, 1995.
Li, G., Okin, S., and Epstein, H. E.: Effects of enhanced wind erosion on surface soil texture and characteristics of windblown sediments, J. Geophys. Res., 114, G02003, doi:10.1029/2008JG000903, 2009
Marticorena, B. and Bergametti, G.: Modeling the atmospheric dust cycle: 1. Design of a soil derived dust emission scheme, J. Geophys. Res., 100, 16415–16430, 1995.
Nickling, W. G. and Gillies, J. A.: Emission of grained particulates from desert soils, in: Pa-

ACPD
11, 11077–11107, 2011

leoclimatology and Paleometeorology: Modern and Past Patterns of Global Atmospheric Transport, edited by: Leinen, M. and Sarnthein, M., 133–165, Kluwer Academic Publishers, Boston, USA, 1989.

Rajot, J. L., Alfaro, S. C., Gomes, L., and Gaudichet, A.: Influence of sandy soil crusting on horizontal and vertical wind erosion fluxes, Catena, 53(1), 1–16, 2003.

Rajot, J. L., Formenti, P., Alfaro, S. C., K. Desboeufs, S., Chevaillier, S., Triquet, B., Chatenet, A., Gaudichet, E., Journet, A., Maman, N., Mouget, A., and Zakou, A.: AMMA dust experiment: An overview of measurements performed during the dry season special observation period (SOP0) at the Banizoumbou (Niger) supersite, J. Geophys. Res., 113, D00C14, doi:10.1029/2008JD009906, 2008.

Sow, M., Alfaro, S. C., Rajot, J. L., and Marticorena, B.: Size resolved dust emission fluxes measured in Niger during 3 dust storms of the AMMA experiment, Atmos. Chem. Phys., 9, 3881–3891, doi:10.5194/acp-9-3881-2009, 2009.

Stout, J. E.: Effect of averaging time one the apparent threshold for Aeolian transport, J. Arid. Environ., 39, 395–401, 1998.

ACPD

11, 11077–11107, 2011

Table 1. Dry size-distribution of the populations of loose soil aggregates present on the surface of the Banizoumbou (Niger) supersite.

	pop 1	pop 2	pop 3
A (%)	21	76	3
σ	1.33	1.62	1.05
gmd (µm)	91	325	3000

ACPD
11, 11077–11107, 2011

Table 2. Main characteristics of the 3 erosion events of the monsoon (ME1, ME4) and convective (CE4) types. For each event the duration (in min), wind direction range (in ° and clockwise with 0° to the north), roughness length (z_0, in mm), wind friction velocity range ($u^*_t u^*_{(}$max), in m s^{-1}), and the parameters (B in %; u^* in m s^{-1}; σ in m s^{-1}) of the statistical distribution of the wind friction velocity values are reported. The contribution (%F_h) of each friction velocity mode to the total saltation flux cumulated over the duration of the events is also indicated. Finally, the loss of fine particles (L, in gm^{-2}) and the average flux ($F_{v,\mathrm{av.}}$, in mgm^{-2} s^{-1}) are given.

Event	ME1	ME4		CE4	
duration	129	39		164	
direction	150–196	220–240		112–210	
z_0	1.70 ± 30%	0.23 ± 24%		3.70 ± 10%	
u^*_t ($u^*_{\max}$)	0.40 (0.57)	0.30 (0.60)		0.45 (0.77)	
u^*distrib.	Mode 1	Mode 1	Mode 2	Mode 1	Mode 2
B (%)	100	61	39	44	56
u^*	0.45	0.33	0.50	0.52	0.67
σ	0.06	0.10	0.03	0.02	0.04
%F$_h$	100	2	98	5	95
L	8.6	3.5		10.5	
$F_{v,\mathrm{av}}$	1.11	1.50		1.01	

ACPD
11, 11077–11107, 2011

Table 3. Results of the deconvolution of the mass and number size-resolved emission fluxes measured during the 2 monsoon (ME1 and ME4) and the convective (CE4) erosion events. In each case the emission flux can be considered as a mixture of 2 or 3 lognormally distributed populations whose amplitudes (A), geometric mean diameters (gmd, in µm), geometric standard deviation (σ), and averages (avg) of these last two parameters are reported. Note that A is expressed in $g\,m^{-2}\,s^{-1}$ in the case of the mass flux, but in particles/$m^2\,s^{-1}$ in the case of the number flux. Values in parenthesis correspond to the proportions of each of the 3 particle populations.

		pop. 1				pop. 2				pop. 3			
		ME1	ME4	CE4	avg	ME1	ME4	CE4	avg	ME1	ME4	CE4	avg
Mass	gmd	2.2	1.5	2.3	*2.0*	4.9	5.1	5.1	*5.0*	10.4	10.4	10	*10.3*
	gsd	1.9	1.8	1.9	*1.9*	1.6	1.7	1.7	*1.7*	1.4	1.5	1.5	*1.5*
	A	7.8E-5	7.1E-5	1.2E-3		1.8E-4	3.4E-4	1.5E-3		2.5E-4	4.4E-4	2.4E-4	
	(%)	(15)	(8)	(41)		(35)	(40)	(51)		(49)	(52)	(8)	
Num.	gmd	0.7	0.6	0.7	*0.7*	2.5	2.1	2.3	*2.3*	7.1	6.1	6.3	*6.5*
	gsd	1.9	1.8	1.9	*1.9*	1.6	1.7	1.7	*1.7*	1.4	1.5	1.5	*1.5*
	A	6.0E6	1.6E7	7.3E7		1.2E6	2.6E6	9.0E6		1.8E5	3.2E5	1.9E5	
	(%)	(81)	(84)	(89)		(17)	(14)	(11)		(2)	(2)	(0)	

ACPD
11, 11077–11107, 2011

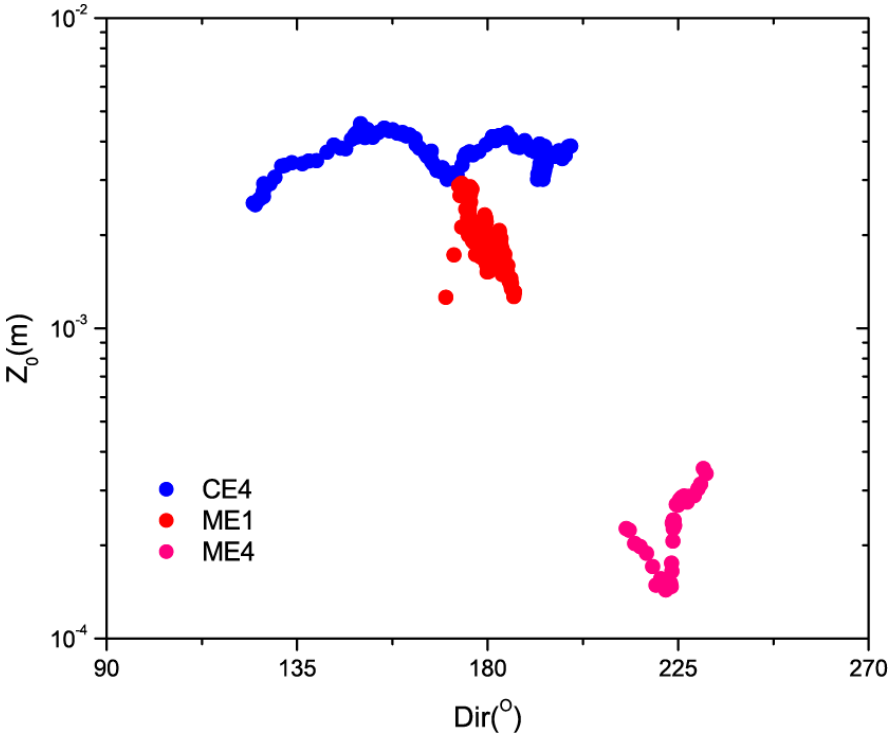

Fig. 1. Variability of the aerodynamic roughness length (z_0) with wind direction for the 3 studied events.

ACPD
11, 11077–11107, 2011

Comparison of the size-resolved dust emission fluxes

M. Sow et al.

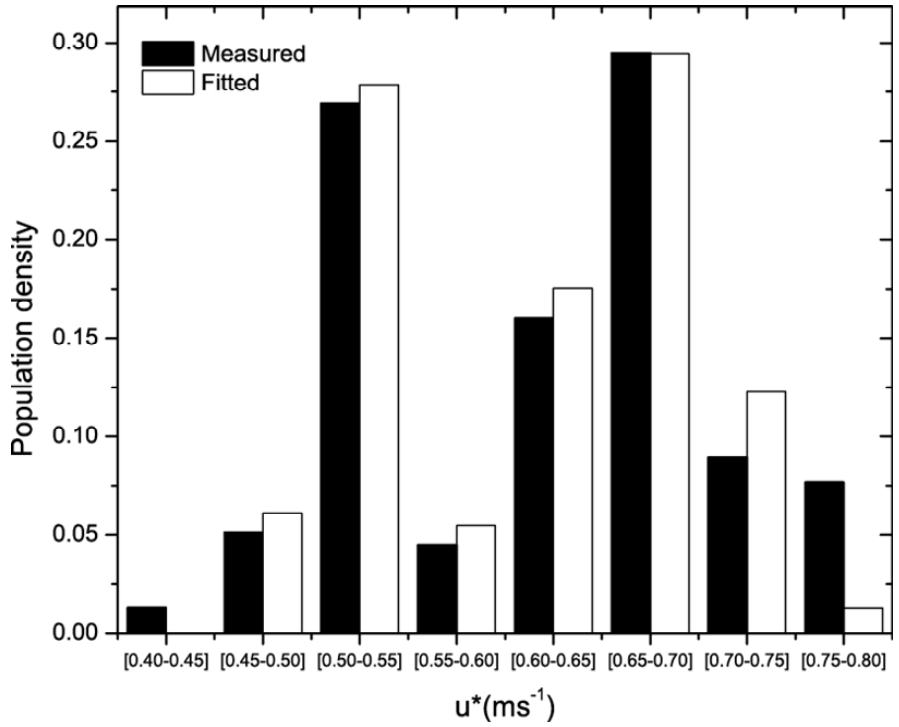

Fig. 2. Statistical distribution of the wind friction velocity values (u^*) measured during the erosion event of the convective type (CE4).

ACPD
11, 11077–11107, 2011

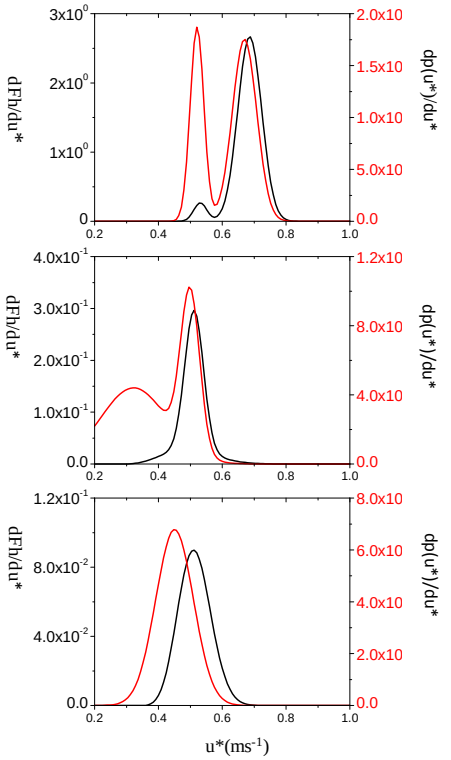

Fig. 3. Statistical distributions of the wind friction velocity for the 3 studied events (red curves) and associated saltation flux density (black curves).

ACPD
11, 11077–11107, 2011

Comparison of the size-resolved dust emission fluxes

M. Sow et al.

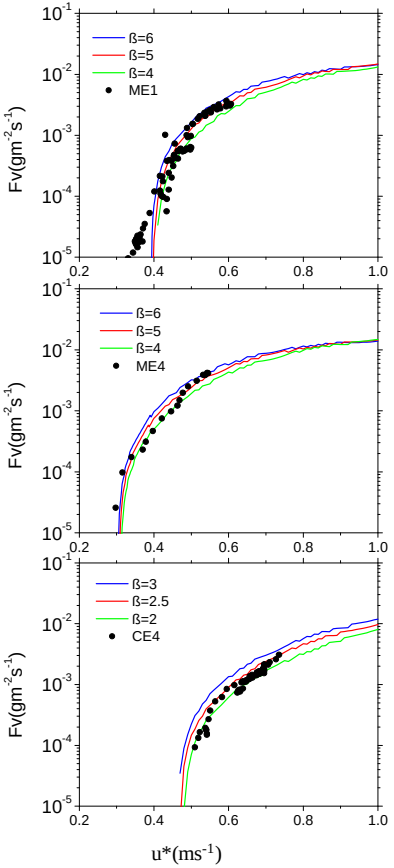

Fig. 4. A fairly good agreement can be obtained between the measured and the calculated mass fluxes. This good agreement is obtained for $\beta = 5$ (± 1) in the case of ME1 and ME4, a value slightly larger than the one previously proposed by Alfaro et al. (2004) but this still >1, which confirms that the binding energies derived from the wind tunnel measurements must be reduced to better reflect the fluxes measured in natural conditions. For CE4, a significantly smaller value ($\beta = 2.5 \pm 0.5$) in better agreement with the previous findings must be selected for the model predictions to match the measurements.

ACPD
11, 11077–11107, 2011

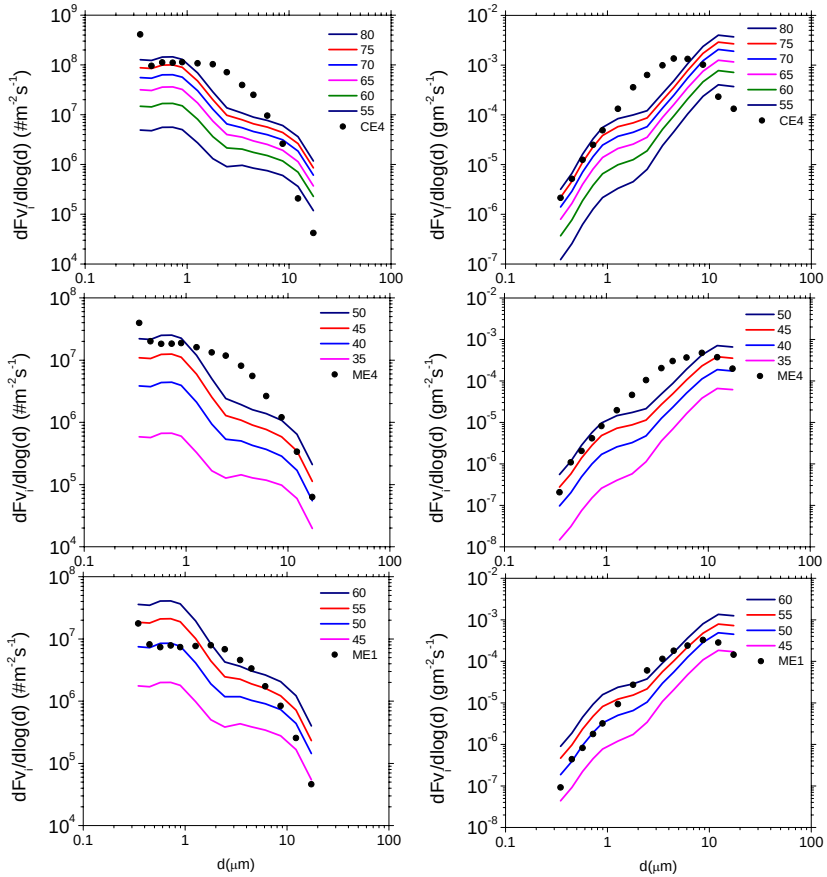

Fig. 5. Comparison of the size-resolved mean flux (black dots) for each event with the DPM predictions for increasing values of u^*. The number and mass fluxes are displayed on the left and right hand sides, respectively.

ACPD
11, 11077–11107, 2011

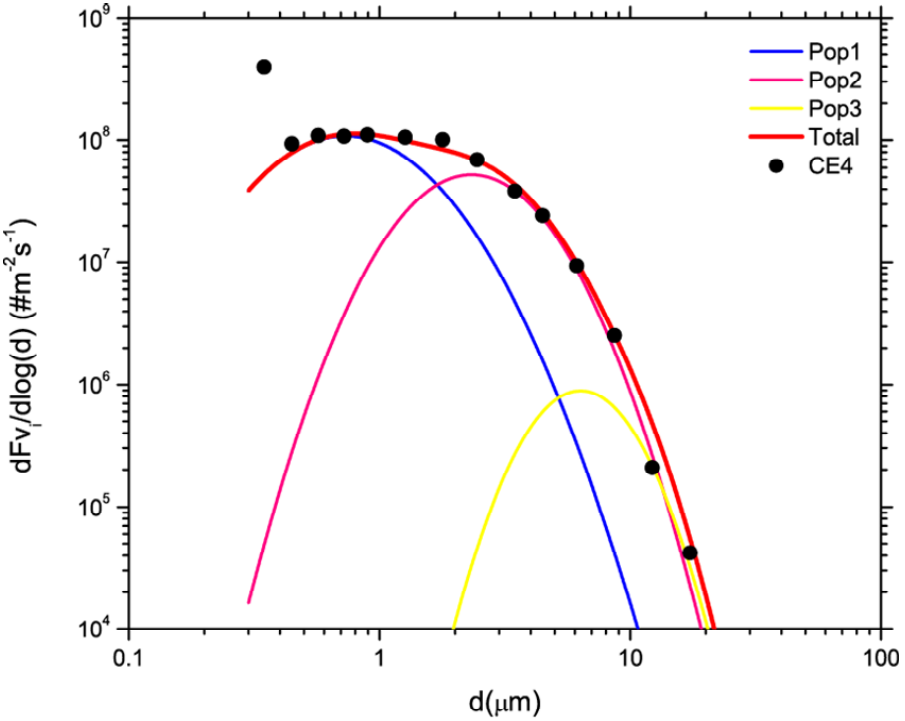

Fig. 6. Illustration of the quality of the deconvolution procedure when a combination (red curve) of 3 log-normal populations is used to fit the measured number flux (black dots). The presented case is for the erosion event of the convective type (CE4).

ACPD
11, 11077–11107, 2011